

Analyzing and characterizing the effects of tDCS on neuronal polarization using biophysically realistic cortical neuron models and head models of E-field

Introduction: Transcranial Direct Current Stimulation (tDCS) has become increasingly popular amongst available stimulation techniques because of its non-invasiveness, safety, portability and affordability. It is widely known that tDCS has many therapeutic benefits such as in treating depression and in treating neuropathic pain after a spinal cord injury [3][5], but little is known about the exact mechanism of action [4][5]. By simulating the effects of tDCS in cranial models validated against theoretical predictions and clinical research data, we can better understand the effects of tDCS on the brain which can lead to improved therapies by optimizing dosages and electrode placement, gain more insight to brain circuitry of neuropathic pain and depression, as well as to extend the use of tDCS for other neurological disorders.

In this project, we aim to simulate the effects of tDCS on biophysically realistic cortical neurons in different cortical layers in order to qualitatively and quantitatively characterize its effect on the brain. We applied uniform E-fields in 266 different orientations to each cortical neuron model at rest to determine which direction produces maximum depolarization of the cell which would suggest greatest increased excitability for the cell since its membrane potential (V_m) will be closer to the firing threshold. Grouping the cells into corresponding cortical layers and comparing the direction of the E-field for maximum polarization provides insight to which cortical layer is most likely to have its firing rate properties altered during a given tDCS stimulation. We then simulated the effects of tDCS on active cortical neurons by injecting different amplitudes of currents into the soma of the cells in the presence of uniform E-fields, in the direction of max polarization, to examine the effect of tDCS on cortical neuron firing rate.

Methods: *Uniform E-field polarization mappings:* A 1V/m, rectangular, 500ms uniform E-field is applied from all possible directions to 25 biophysically realistic neuron models created by Abera et al. that consist of layers 1-6 for spatial effects and 5 neurons with different morphologies in each layer shown in Figure 1 [1]. The polarization of the soma, dendrites, and axons of each neuron is then recorded. A uniform E-field is used as an approximate of the E-field

generated by tDCS that each neuron experiences. We chose to use a rectangular waveform since it is a simple waveform and commonly used for tDCS (some include a ramp up/down).

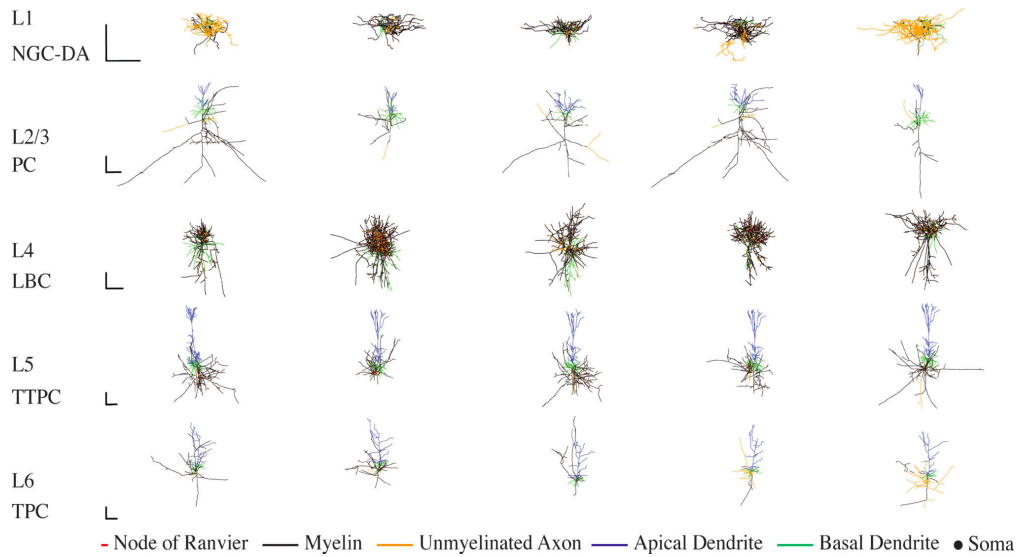


Figure 1: Morphology of model cortical neurons by Aberra et al. Scale bar = 250 μ m.

Simulating the effects of tDCS on the firing properties of the cell: To imitate the normal activity and excitability of the cortical neurons without tDCS, we injected different amounts of current, ranging from 0nA - 1nA, 2nA, or 4nA depending on the cortical layer, with 1.5sec pulse duration, into the soma of the 25 biophysically realistic neuron models, and their firing frequencies are calculated and recorded as control. The neuron models are placed in a 37-degree Celsius environment. The current - frequency relationship is validated against experimental data (Figure 2) [8][9]. Then, a 1V/m, 5V/m, and 10V/m uniform E-field in the direction of peak median somatic polarization is applied to the 25 biophysically realistic neurons and the firing frequency is recorded to compare with the control.

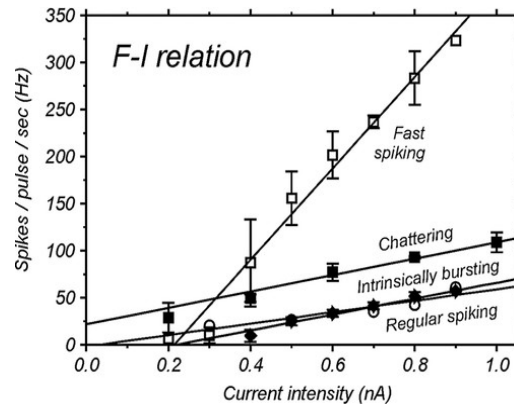


Figure 2: Experimental frequency - current relationship for neurons in cat PVC, characterized by firing type (Fast Spiking, Regular Spiking, Intrinsic Bursting, Chattering) [8]

Results: Uniform E-field polarization mappings. To visualize the response of the soma, dendrites, and axons of neurons in the cortex in a uniform E-field, we generated two types of plots: 1) The Mollweide projection plot represents response at all possible E-field angles and is used for easy visualization of the direction of maximum polarization. Hyperpolarized compartments are in blue, and polarized compartments are in red. The greater the amplitude of polarization, the darker the color, and the maximum polarized compartment is marked by a star. 2) The scatter plot plots polarization versus cortical layer at three different angle ranges (0-60, 65-120, 125-180 degrees with respect to the normal vector of the scalp). This plot allows analysis of the distribution of polarization in the 5 neurons with different morphology in each cortical layer, as well as the difference across E-field directions.

Characterization of Somatic Response to Uniform E-field: Layers 2/3, 5, and 6 tend to show somatic depolarization when exposed to a downward uniform electric field, somatic hyperpolarization when exposed to an upward electric field, and relatively no polarization when exposed to a tangential electric field, whereas Layers 1 and 4 tend to show more variability (Figure 3). A quantitative analysis shows that the soma tended to become hyperpolarized when exposed to an upwards E-field with medians ranging from $-200\mu\text{V}$ to $-40\mu\text{V}$, depolarized when exposed to a downward electric field with medians ranging from $40\mu\text{V}$ to $200\mu\text{V}$, and maintain its polarization when exposed to a transverse electric field with medians ranging from $-5\mu\text{V}$ to $30\mu\text{V}$ (Figure 5). In addition, for upwards E-fields, the maximum polarization ranged from -

100 μ V to -50 μ V between cells, for transverse E-fields, the maximum polarization ranged from -5 μ V to 200 μ V, and for downwards E-fields, the maximum ranged from 0-150 μ V.

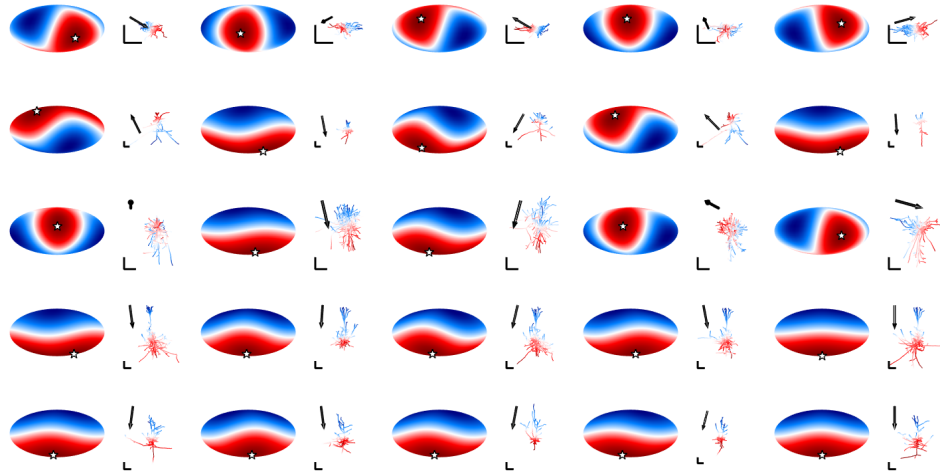


Figure 3: Normalized Mollweide Projection of Somatic Polarization: Note each row corresponds to 5 different cells from a distinct neural layer starting from L1 nucleus gigantocellularis (NGC) neurons (top row), L2/3 pyramidal cells (PC), L4 Large Basket Cells (LBC), L5 PC, L6 PC (bottom row).

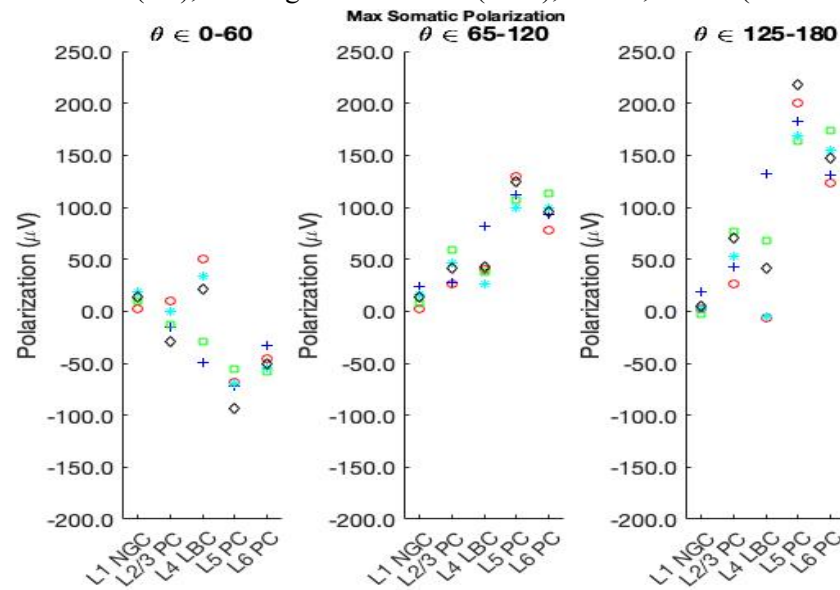


Figure 4: Scatter plot of Max Somatic Polarization for Clone Cells in Each Cortical Layer
Theta values between 0-60 were categorized as an upwards electric field, from 65-120 as transverse, and 125-180 as downward.

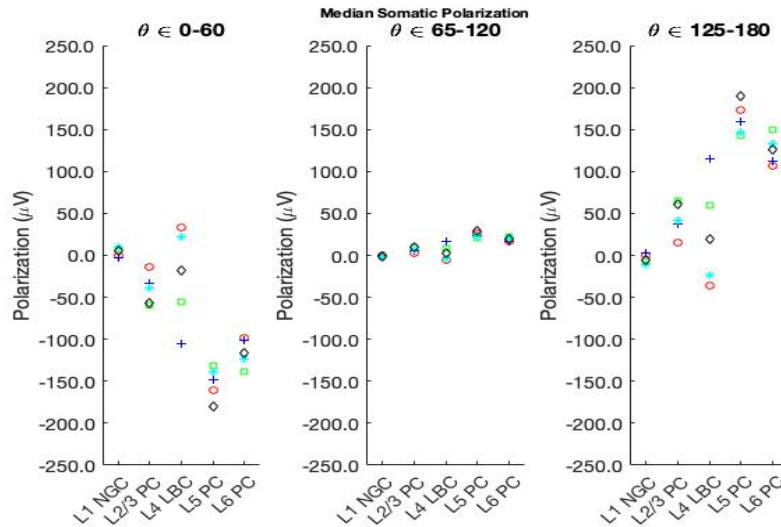


Figure 5: Scatter plot of *Median Somatic Polarization* for Different Cells in Each Cortical Layer

Characterization of Dendritic Response to Uniform E-field: The maximum absolute polarization for dendrites in response to an applied E-field appears to occur in the dendritic terminals as shown in Figure 6. When exposed to an upward E-field, the median polarization for dendritic compartments of L1 NGC cells ranged between $-20\mu\text{V}$ to $25\mu\text{V}$, of L2/3 PC ranged between $-50\mu\text{V}$ to $40\mu\text{V}$, of L4 LBC ranged between $-70\mu\text{V}$ to $25\mu\text{V}$, of L5 PC ranged between $-100\mu\text{V}$ to $-60\mu\text{V}$, and of L6 PC ranged between $-60\mu\text{V}$ to $-25\mu\text{V}$. In addition, the maximum depolarization for dendritic compartments of L1 NGC cells ranged between $.08\text{mV}$ to $.18\text{mV}$, of L2/3 PC ranged between $.3\text{mV}$ to $.4\text{mV}$, of L4 LBC ranged between 0.2mV to 0.35mV , of L5 PC ranged between 0.4mV to 0.5mV , and of L6 PC ranged between 0.30mV to 0.35mV .

When exposed to an downward E-field, the median polarization for dendritic compartments of L1 NGC cells ranged between $-20\mu\text{V}$ to $20\mu\text{V}$, of L2/3 PC ranged between $-40\mu\text{V}$ to $50\mu\text{V}$, of L4 LBC ranged between $-25\mu\text{V}$ to $75\mu\text{V}$, of L5 PC ranged between $60\mu\text{V}$ to $100\mu\text{V}$, and of L6 PC ranged between $30\mu\text{V}$ to $60\mu\text{V}$. In addition, the maximum depolarization for dendritic compartments of L1 NGC cells ranged between $.05\text{mV}$ to $.25\text{mV}$, of L2/3 PC ranged between $.15\text{mV}$ to $.30\text{mV}$, of L4 LBC ranged between 0.30mV to 0.60mV , of L5 PC ranged between 0.35mV to 0.45mV , and of L6 PC ranged between 0.25mV to 0.35mV .

When exposed to a transverse E-field, the median polarization for dendritic compartments for cells was about $0\mu\text{V}$, ranging from $-5\mu\text{V}$ to $20\mu\text{V}$. In addition, the maximum depolarization for dendritic compartments of L1 NGC cells ranged between .10mV to .25mV, of L2/3 PC ranged between .25mV to .35mV, of L4 LBC ranged between 0.30mV to 0.45mV, of L5 PC ranged between 0.30mV to 0.40mV, and of L6 PC ranged between 0.25mV to 0.30mV.

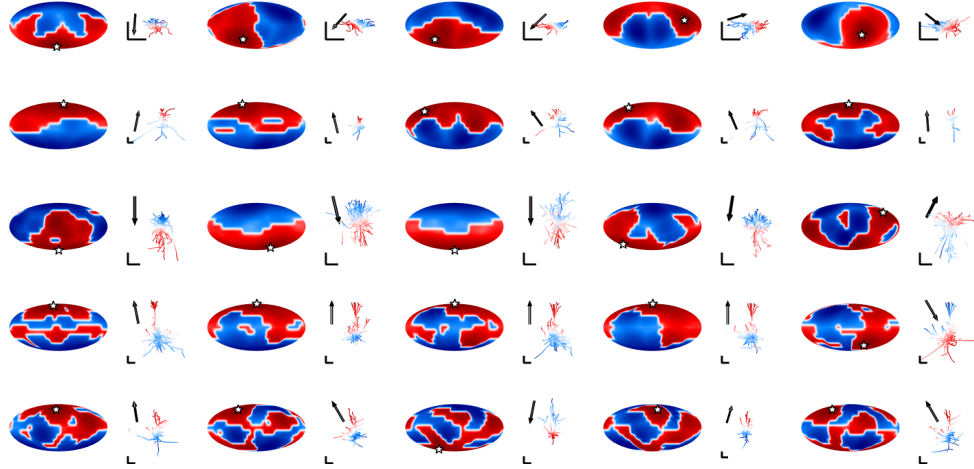


Figure 6: *Normalized Mollweide Projection of the Max Absolute Value for Dendritic Compartments:* Note this plot looks for the max absolute value in polarization across all compartments. The sharp change from polarization to hyperpolarization is because a small change in orientation of the E-field may cause the abs. value of a compartment in another branch to be of greater magnitude and may be different sign.

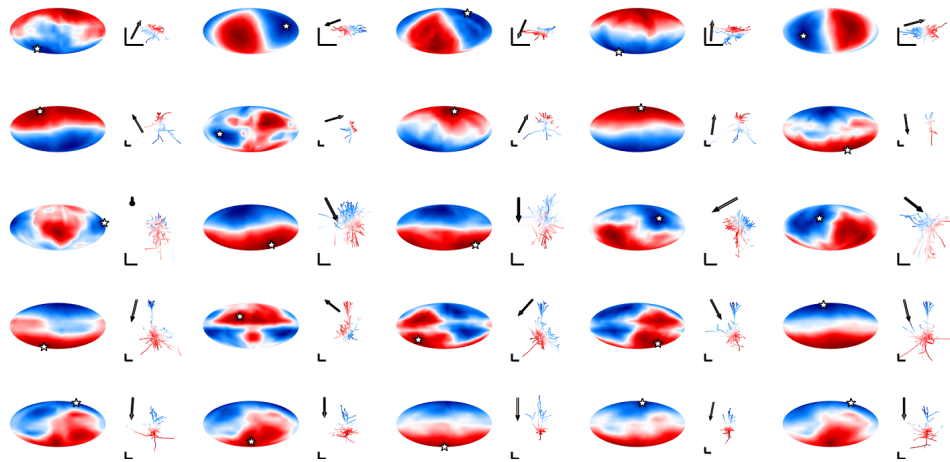


Figure 7: *Normalized Mollweide Projection of the Median for Dendritic Compartments*

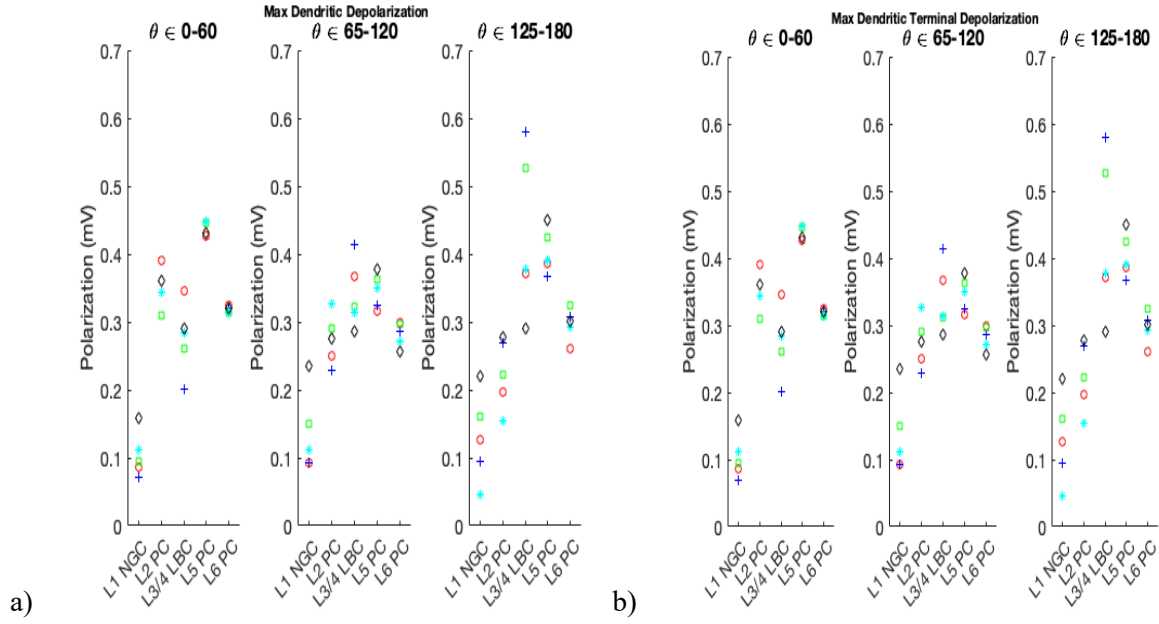


Figure 8: a) Scatter plot of **Max Dendritic Polarization** for Different Cells in Each Cortical Layer
b) Scatter plot of **Max Dendritic Terminal Polarization** for Different Cells in Each Cortical Layer

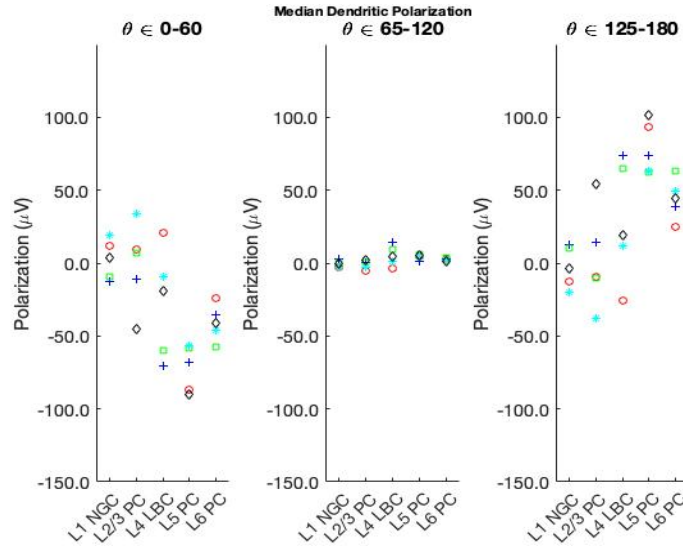


Figure 9: Scatter plot of **Median Dendritic Polarization** for Different Cells in Each Cortical Layer

Characterization of Axonal Response to Uniform E-field: The maximum absolute polarization for axonal in response to an applied E-field appears to occur in the axonal terminals as shown in Figure 10. When exposed to an upward E-field, the median polarization for axonal compartments of L1 NGC cells ranged between $-10\mu V$ to $0\mu V$, of L2/3 PC ranged between $-300\mu V$ to $-200\mu V$, of L4 LBC ranged between $0\mu V$ to $100\mu V$, of L5 PC ranged between $-300\mu V$ to $-100\mu V$, and of

L6 PC ranged between $-150\mu\text{V}$ to $150\mu\text{V}$. In addition, the maximum depolarization for axonal compartments of L1 NGC cells ranged between $.20\text{mV}$ to $.30\text{mV}$, of L2/3 PC ranged between $.35\text{mV}$ to $.60\text{mV}$, of L4 LBC ranged between 0.25mV to 0.45mV , of L5 PC ranged between 0.35mV to 0.6mV , and of L6 PC ranged between 0.30mV to 0.45mV .

When exposed to an downward E-field, the median polarization for axonal compartments of L1 NGC cells ranged between $0\mu\text{V}$ to $10\mu\text{V}$, of L2/3 PC ranged between $110\mu\text{V}$ to $350\mu\text{V}$, of L4 LBC ranged between $-100\mu\text{V}$ to $0\mu\text{V}$, of L5 PC ranged between $150\mu\text{V}$ to $300\mu\text{V}$, and of L6 PC ranged between $-200\mu\text{V}$ to $-100\mu\text{V}$. In addition, the maximum depolarization for axonal compartments of L1 NGC cells ranged between $.20\text{mV}$ to $.25\text{mV}$, of L2/3 PC ranged between $.60\text{mV}$ to $.80\text{mV}$, of L4 LBC ranged between 0.30mV to 0.60mV , of L5 PC ranged between 0.30mV to 0.80mV , and of L6 PC ranged between 0.35mV to 0.55mV .

When exposed to a transverse E-field, the median polarization for axonal compartments for cells was about $0\mu\text{V}$, ranging from $-50\mu\text{V}$ to $50\mu\text{V}$. In addition, the maximum depolarization for axonal compartments of L1 NGC cells ranged between $.25\text{mV}$ to $.3\text{mV}$, of L2/3 PC ranged between $.45\text{mV}$ to $.70\text{mV}$, of L4 LBC ranged between 0.25mV to 0.55mV , of L5 PC ranged between 0.35mV to 0.80mV , and of L6 PC ranged between 0.30mV to 0.60mV .

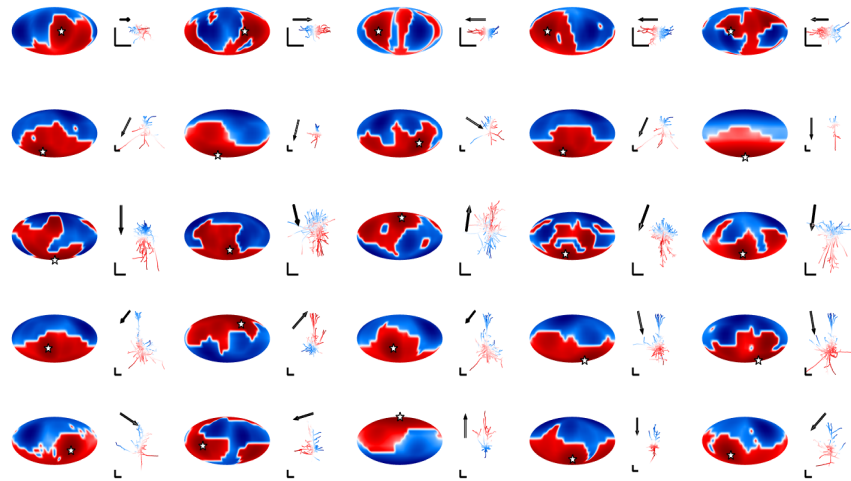


Figure 10: Normalized Mollweide Projection of the *Max Absolute Value for Axonal Compartments*

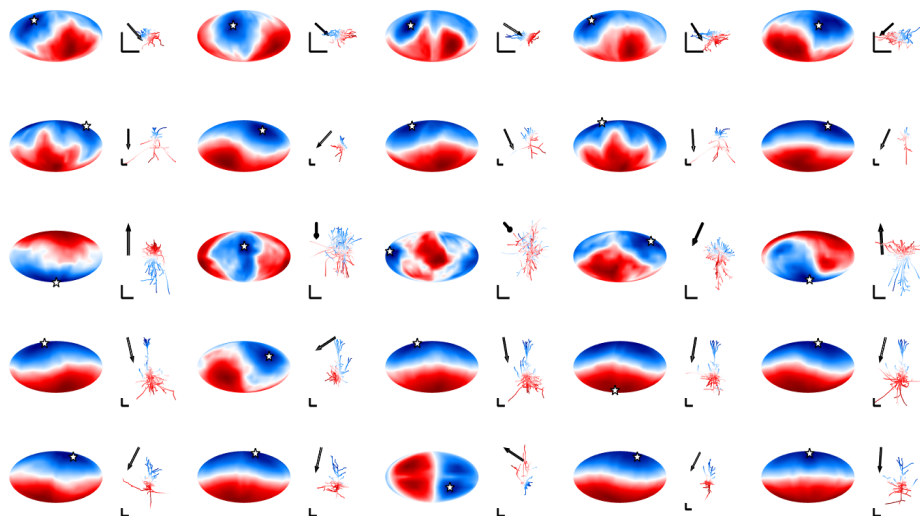


Figure 11: Normalized Mollweide Projection of the *Median Axon Terminal Compartments*

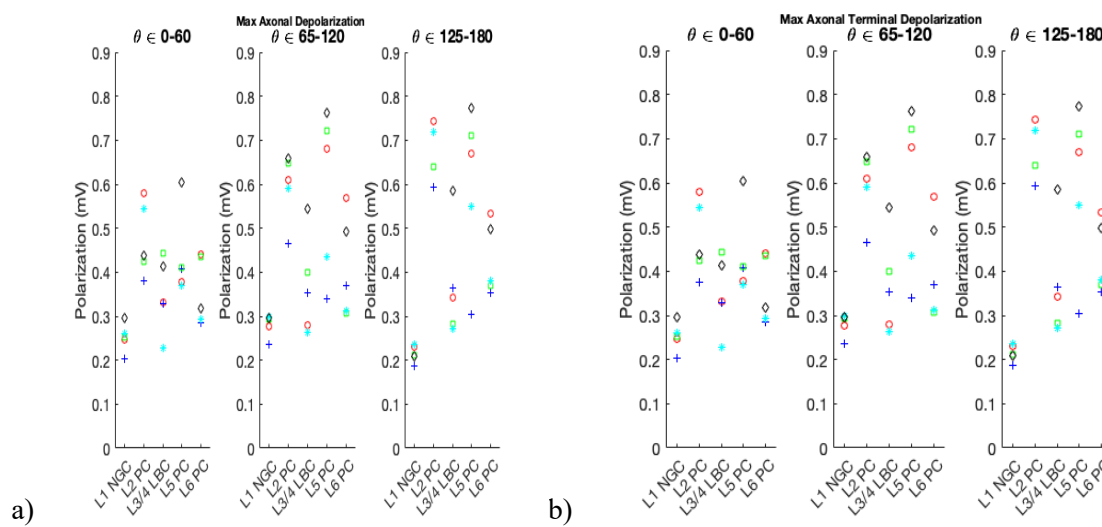


Figure 12: a) Scatter plot of *Max Axonal Polarization* for Different Cells in Each Cortical Layer
b) Scatter plot of *Max Axonal Terminal Polarization* for Different Cells in Each Cortical Layer

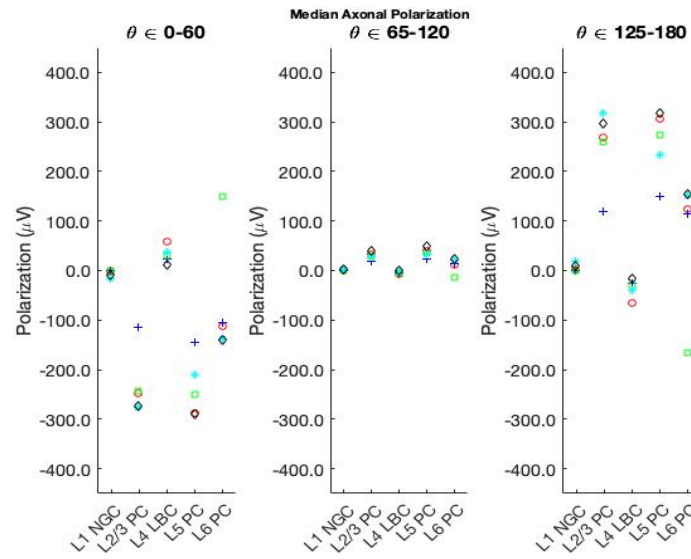


Figure 13: Scatter plot of **Median Axonal Polarization** for Different Cells in Each Cortical Layer

Effects of tDCS on the firing properties of the cell:

Current injections to simulate existing brain activity: Layer 1 had a maximum frequency of 191.3 Hz at 2nA followed by Layer 4 with a maximum frequency of 84 Hz at nA. Layers 2,3, 5 and 6 all had about half a magnitude smaller frequency, with max frequencies ranging between 20-40. The results obtained matching several *in vivo* and as well as computational results in cat [1][8][9]. A 1V/m uniform E-field was then applied to simulate tDCS in the direction of maximum median polarization, maximum somatic polarization, maximum dendritic polarization, and maximum axonal polarization and no change in firing rate was observed.

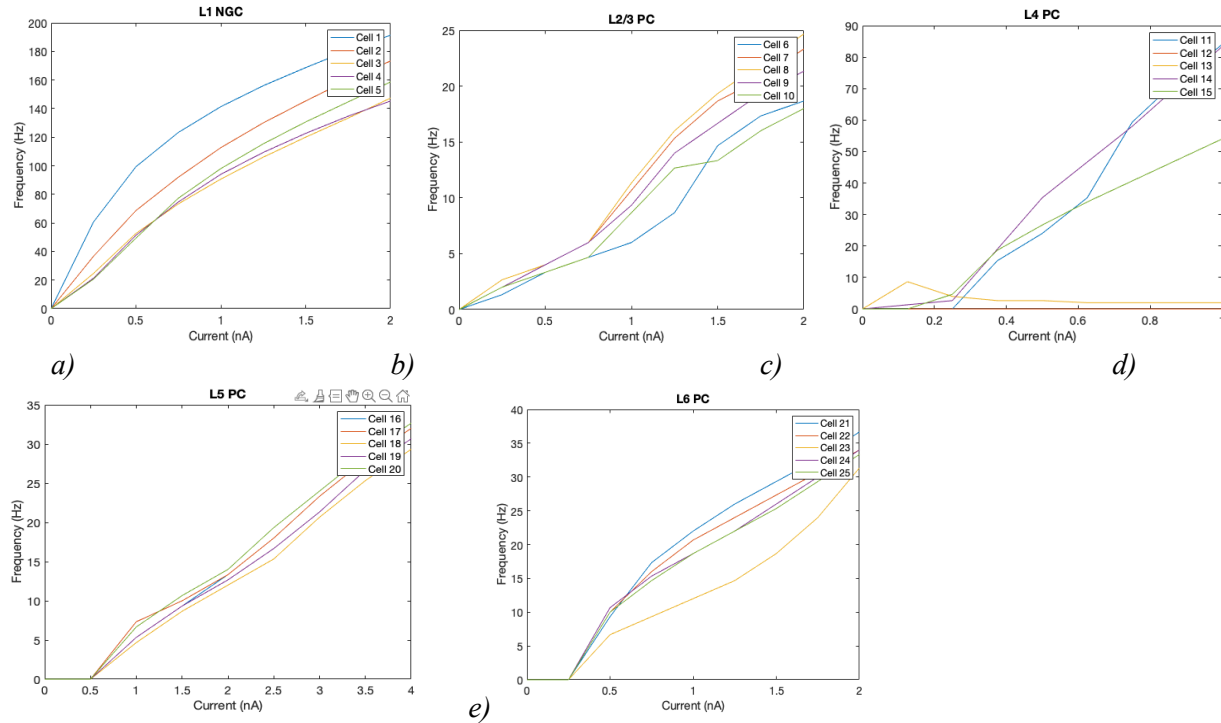


Figure 14: **a)** Frequency-current (F-I) Curve for L1 NGC cells **b)** Frequency-current (F-I) Curve for L2/3 Pyramidal Cells **c)** Frequency-current (F-I) Curve for L4 Pyramidal Cells **d)** Frequency-current (F-I) Curve for L5 Pyramidal Cells **e)** Frequency-current (F-I) Curve for L6 Pyramidal Cells

Discussion:

Somatic Polarization: For all layers, the excitability of the soma is about the same for both upwards and downwards E-fields but is about 0 for E-field parallel to the scalp. Soma of neurons in Layers 5 and 6 were found to be the most excitable. **Dendrite summary:** The sites of maximum hyperpolarization/depolarization tends to occur in the dendritic terminals. This can be explained by the cable theory where V_m becomes dependent on E-field magnitude instead of E-field gradient at a geometrical discontinuity--terminal, which is much more sensitive to change in E-field than the rest of the dendrite [1][6][7]. Layer 1 neurons tend to have the smallest max depolarization, and have almost zero excitability in any E-field direction. The max depolarization/hyperpolarization of dendrites is less dependent on field direction than soma. Excitability of dendrites in different layers is similar to that of the soma. Layers 5 and 6 tend to have their dendritic compartments depolarized when exposed to a downward electric field, as well as Layer 4 with some slight variability, whereas no noticeable trend exists for Layers 1-3.

Axon Summary: The sites of maximum hyperpolarization/depolarization tend to occur in the axonal terminals. This again can be explained by the cable theory used for dendritic terminals. Layers 5 and 6 tend to have axonal compartments depolarized when exposed to a downward electric field, as well as Layer 4 with some slight variability, whereas no noticeable trend exists for Layers 1-3. Max axonal depolarization occurs with either a parallel or a downward E-field, and max axonal hyperpolarization occurs with either parallel or outward E-field. Axons in Layer 1 are almost non-excitabile, Layers 2-6 have similar excitability in upward and downward fields.

Comparison Between Compartment Types: The same median polarization pattern persists when comparing the same cell's different compartment types (i.e. when comparing median axonal, dendritic, and somatic polarization), just with different magnitudes. Layers 5 and 6 tend to be depolarized when applied to a downward uniform E-field and hyperpolarized when applied to an upward uniform E-field, with Layer 4 having some slight variability but the same general pattern. **Firing rate:** When a 1V/m uniform E-field was applied in the directions of maximum depolarization in the soma, axon, and dendrite, the same firing rate pattern was exhibited, suggesting that it had no effect on the firing rate properties of the cell. Future work needs to be done by using both uniform E-fields with a higher amplitude to gain a better understanding of how tDCS affects the brain as well as with FEM generated E-fields with higher amplitudes to capture a more realistic clinical setting. In addition, synaptic inputs need to be incorporated to capture more of the effects that tDCS has on the brain.

Conclusion: In conclusion, this project introduces a simulation protocol for determining the response to tDCS on biophysically realistic cortical neurons, but more work needs to be done. By combining the above future experiments in junction with the work provided here, we hope that this work provides a basis for the continued mechanistic studies for tDCS therapies.

Sources:

- [1]Aberra, A. S., Peterchev, A. V., & Grill, W. M. (2018). Biophysically realistic neuron models for simulation of cortical stimulation. *Journal of Neural Engineering*, 15(6), 066023. doi: 10.1088/1741- 2552/aadbb1
- [2]Aberra, A., Wang, B., Grill, W. M., & Peterchev, A. V. (2018). Simulation of transcranial magnetic stimulation in head model with morphologically-realistic cortical neurons. doi: 10.1101/506204
- [3]Soler, M. D.; Kumru, H.; Pelayo, R.; Vidal, J.; Tormos, J. M.; Fregni, F.; Navarro, X.; Pascual-Leone, A. (2010-09-01). "Effectiveness of transcranial direct current stimulation and visual illusion on neuropathic pain in spinal cord injury". *Brain*. 133(9): 2565–2577. doi:10.1093/brain/awq184. ISSN 0006-8950. PMC 2929331. PMID 20685806.
- [4]Nitsche M, et al, (2009) Treatment of depression with transcranial direct current stimulation (tDCS): A Review *Experimental Neurology* <https://doi.org/10.1016/j.expneurol.2009.03.038>
- [5]Hultman, Rainbo, Kyle Ulrich, Benjamin D. Sachs, Cameron Blount, David E. Carlson, Nkemdilim Ndubizu, Rosemary C. Bagot, et al. "Brain-wide Electrical Spatiotemporal Dynamics Encode Depression Vulnerability." *Cell* 173, no. 1 (March 22, 2018): 166-180.e14. <https://doi.org/10.1016/j.cell.2018.02.012>.
- [6]Ranck J B 1975 Which elements are excited in electrical stimulation of mammalian central nervous system: a review. *Brain Res*
- [7]Nagarajan S S, Durand D M and Warman E N 1993 Effects of induced electric fields on finite neuronal structures: a simulation study *IEEE Trans. Biomed. Eng*
- [8]Nowak LG, Azouz R, Sanchez-Vives MV, Gray CM, and McCormick DA. Electrophysiological classes of cat primary visual cortical neurons in vivo as revealed by quantitative analyses. *J Neurophysiol* 89: 1541–1566, 2003.
- [9]Tateno T, Harsch A, Robinson HP. Threshold firing frequency-current relationships of neurons in rat somatosensory cortex: type 1 and type 2 dynamics. *J Neurophysiol* 92: 2283–2294, 2004. doi:10.1152/jn.00109.2004.